Development 139, 3343-3354 (2012) doi:10.1242/dev.075465

Antagonism of Nodal signaling by BMP/Smad5 prevents ectopic primitive streak formation in the mouse amnion

Paulo N. G. Pereira[1], Mariya P. Dobreva[1], Elke Maas[1], Frederique M. Cornelis[1], Iván M. Moya[1], Lieve Umans[2,*], Catherine M. Verfaillie[3], Anne Camus[4], Susana M. Chuva de Sousa Lopes[5], Danny Huylebroeck[2,*] and An Zwijsen[1,‡]

SUMMARY

The strength and spatiotemporal activity of Nodal signaling is tightly controlled in early implantation mouse embryos, including by autoregulation and feedback loops, and involves secreted and intracellular antagonists. These control mechanisms, which are established at the extra-embryonic/embryonic interfaces, are essential for anterior-posterior patterning of the epiblast and correct positioning of the primitive streak. Formation of an ectopic primitive streak, or streak expansion, has previously been reported in mutants lacking antagonists that target Nodal signaling. Here, we demonstrate that loss-of-function of a major bone morphogenetic protein (BMP) effector, Smad5, results in formation of an ectopic primitive streak-like structure in mutant amnion accompanied by ectopic *Nodal* expression. This suggests that BMP/Smad5 signaling contributes to negative regulation of *Nodal*. In cultured cells, we find that BMP-activated Smad5 antagonizes Nodal signaling by interfering with the Nodal-Smad2/4-Foxh1 autoregulatory pathway through the formation of an unusual BMP4-induced Smad complex containing Smad2 and Smad5. Quantitative expression analysis supports that ectopic *Nodal* expression in the *Smad5* mutant amnion is induced by the Nodal autoregulatory loop and a slow positive-feedback loop. The latter involves BMP4 signaling and also induction of ectopic *Wnt3*. Ectopic activation of these *Nodal* feedback loops in the *Smad5* mutant amnion results in the eventual formation of an ectopic primitive streak-like structure. We conclude that antagonism of Nodal signaling by BMP/Smad5 signaling prevents primitive streak formation in the amnion of normal mouse embryos.

KEY WORDS: Amnion, Bone Morphogenetic Protein, Nodal, Primitive streak, Smad, Mouse

INTRODUCTION

Cell fate is determined by intrinsic programs and external cues, such as growth factors, cell-cell contacts and cell-matrix contacts. In the early embryo, Nodal and BMPs are morphogens that play pivotal roles in gastrulation and tissue patterning. These ligands belong to the transforming growth factor (TGF) type β family. Nodal and BMPs present frequently opposing roles during fate determination, as demonstrated in several cellular and developmental contexts, such as in differentiation of mouse embryonic stem cells (Fei and Chen, 2010; Galvin et al., 2010) or in patterning of the nascent mesoderm in the primitive streak during the gastrula stage of mouse development (Tam and Loebel, 2007; Willems and Leyns, 2008). In the primitive streak, epiblast cells ingress while undergoing an epithelial-to-mesenchymal transition (EMT), and form mesoderm and definitive endoderm. While BMP signaling is required for specification of derivatives formed at the posterior part of the primitive streak (Bachiller et al., 2000; Kalantry et al., 2001; Lawson et al., 1999; Winnier et al., 1995), increasingly higher Nodal signaling is required for specification of derivatives formed at the anterior part of the primitive streak (Norris et al., 2002; Vincent et al., 2003).

Nodal and BMP also function cooperatively during, for example, formation of the primitive streak. Robust *Nodal* expression (and signaling) is required for primitive streak formation and its correct positioning is triggered by the *Nodal* autoregulatory loop and amplified via the slow positive-feedback loop, which requires *Bmp4* and *Wnt3* expression and signaling (Ben-Haim et al., 2006; Shen, 2007). High levels of Nodal signaling are required for specification and allocation of the anterior visceral endoderm (AVE) (Mesnard et al., 2006; Norris et al., 2002; Yamamoto et al., 2001a). The latter tissue secretes antagonists of Nodal, BMP and Wnt signaling, namely Cerberus-like (Cer1), Dickkopf-related protein 1 (Dkk1) and Lefty1, which restrict the mesoderm-inducing signals to the prospective posterior side of the embryo where the primitive streak is formed (Kimura et al., 2000; Perea-Gomez et al., 2002).

The binding of Nodal ligand to the Alk4 and ActRIIA/ActRIIB receptor complex activates the downstream effectors, or receptor-regulated Smads (R-Smads), Smad2 and Smad3 (Sakuma et al., 2002). Binding of BMPs to receptor complexes activates another subset of R-Smads, namely Smad1, Smad5 and Smad8 (Kawai et al., 2000; Meersseman et al., 1997). Unique to the Nodal system is the crucial requirement of a co-receptor from the EGF-CFC family – Cripto and Cryptic (Ding et al., 1998). Activated R-Smads form heteromeric complexes with the common Smad (Smad4), translocate into the nucleus and regulate, in combination with other transcription factors and co-factors, the transcription of target genes. In the case of Nodal signaling, activated Smad complexes interact with transcription factors such as Mixl1 and Foxh1 (Shi

[1]Laboratory of Developmental Signaling of the VIB11 Center for the Biology of Disease, VIB, and Center for Human Genetics, KU Leuven, B-3000 Leuven, Belgium. [2]Laboratory of Molecular Biology (Celgen) of the Department of Molecular and Developmental Genetics, VIB, and Center for Human Genetics, KU Leuven, B-3000 Leuven, Belgium. [3]Interdepartmental Stem Cell Institute Leuven, KU Leuven, B-3000 Leuven, Belgium. [4]Université Paris-Diderot, CNRS, Institut Jacques Monod, Paris 75013, France. [5]Department of Anatomy and Embryology, Leiden University Medical Center, Leiden 2333 ZC, The Netherlands.

*Present address: Department of Development and Regeneration, KU Leuven, B-3000 Leuven, Belgium
‡Author for correspondence (an.zwijsen@cme-vib.kuleuven.be)

Accepted 18 June 2012

and Massague, 2003). The Nodal-Smad2/4-Foxh1 cascade induces *Nodal* expression itself (the Nodal autoregulatory loop), and also establishes a negative regulatory loop by the direct induction of the Nodal antagonist *Lefty2* (Hoodless et al., 2001; Yamamoto et al., 2001a). The Lefty proteins are TGFβ family ligands that compete extracellularly with Nodal and its (co-)receptors, and hence interfere via different modes with the activation of the Nodal signaling cascade (Chen and Shen, 2004; Cheng et al., 2004; Sakuma et al., 2002; Tanegashima et al., 2004).

Crosstalk and genetic interaction between Nodal and BMP signaling pathways has been demonstrated in different developmental contexts where these ligands co-signal in zebrafish, *Xenopus* and mice (Chocron et al., 2007; Yamamoto et al., 2001b). BMP signaling attenuates Nodal signaling and expression during left-right (LR) axis determination in mouse embryos (Chang et al., 2000; Furtado et al., 2008; Mine et al., 2008). Smad1-mediated BMP signaling sets a repressive threshold for Nodal signaling in the left lateral plate mesoderm (LPM) by limiting the availability of Smad4. This attenuates Nodal signaling and establishes a robust, but not exceedingly high, level of signaling during LR axis determination (Furtado et al., 2008). Mice lacking *Smad5* express *Nodal* bilaterally in the LPM instead of unilaterally in left LPM, and the expression of the Nodal target genes *Pitx2*, *Lefty1* and *Lefty2* was affected (Chang et al., 2000). Even though *Smad1* and *Smad5* mutant mice have similar LR asymmetry defects associated with altered Nodal signaling, it remains unclear whether and how Smad5 signaling antagonizes Nodal signaling.

Smad1 and Smad5 share striking sequence homology and their mRNA is fairly ubiquitously expressed in the embryo proper. *Smad1* (Lechleider et al., 2001; Tremblay et al., 2001) or *Smad5* (Chang et al., 1999; Yang et al., 1999) loss-of-function mouse mutants or compound heterozygosity of *Smad1* and *Smad5* (Arnold et al., 2006) are all embryonic lethal. The conventional *Smad5* knockouts die around mid-gestation from several embryonic and extra-embryonic defects that can be attributed to reduced BMP signaling. Amnion closure is delayed in the *Smad5* mutant, which resembles a milder phenotype of the *Bmp2* mutant mice (Zhang and Bradley, 1996). The amnion is normally a thin and avascular extra-embryonic tissue that forms from a single amniochorionic fold during gastrulation and ultimately surrounds and cushions the fetus (Pereira et al., 2011). After amnion closure, the *Smad5* mutant amnion develops specific defects that cannot be attributed to reduced BMP signaling (Bosman et al., 2006). The cells of the amniotic ectoderm are cuboidal in the anterior part of the *Smad5* mutant amnion, and the anterior delineation between neural, surface and amnion ectoderm is lost. At early somite stages, mutant amniotic ectoderm and mesoderm thicken anteriorly, resulting in a clump of cells. The amniotic clump displays ectopic hematopoiesis and vasculogenesis, and develops de novo PGC-like cells. These different mesodermal cells normally form at the posterior part of the primitive streak. These cells are stereotypically organized within the clump of cells in the *Smad5* mutant amnion. Increased or ectopic *Bmp* and target gene expression in the mutant amnion suggest that lack of *Smad5* results in a gain-of-function of BMP signaling in the amnion (Bosman et al., 2006). Given that the thickened amnion contains mesoderm cell types normally specified in the posterior part of the primitive streak, we investigated whether an ectopic primitive streak is induced. Knowing that Nodal signaling is crucial for establishment of the primitive streak and that this function is highly conserved (Shen, 2007; Tian and Meng, 2006), we questioned whether Smad5-mediated signaling is required in the mouse embryo to antagonize Nodal signaling and to prevent ectopic primitive streak formation in amnion.

Here, we find that the formation of a primitive streak-like structure in *Smad5* mutant amnion is accompanied by ectopic *Nodal* expression. Biochemical studies in cells demonstrate that Smad5-mediated BMP signaling interferes with the Nodal autoregulatory loop. Comparative quantitative gene expression analysis is compatible with ectopic *Nodal* in the *Smad5*-deficient amnion being induced via the Nodal autoregulatory loop and amplified via the slow positive-feedback loop. We propose that Smad5-mediated antagonism of Nodal signaling in the amnion is an essential mechanism to prevent primitive streak formation in this extra-embryonic tissue.

MATERIALS AND METHODS

Mice

Smad5$^{m1/m1}$ is a conventional *Smad5* knockout mouse (Chang et al., 1999). In *Nodal*$^{lacZ/+}$ mice, one *Nodal* allele is replaced by cDNA encoding β-galactosidase (Varlet et al., 1997). *BAT-gal* mice express *lacZ* under control of canonical Lef/Tcf-dependent Wnt signaling (Maretto et al., 2003). *BRE-lacZ* mice express *lacZ* under control of the BMP responsive element (BRE) from the *Id1* promoter region (Monteiro et al., 2004). All experiments were approved by the ethical commission from KU Leuven (097/2008).

Whole-mount in situ hybridization, β-galactosidase staining and immunohistochemistry

Whole-mount in situ hybridization was performed using standard procedures (Rosen and Beddington, 1993) with antisense probes for the following genes: *T* (Herrmann et al., 1990), *Cer1* (Belo et al., 1997), *Dlx5* (Yang et al., 1998), *Dkk1* (J. Debruyn, KU Leuven, Belgium), *Eomes* (Ciruna and Rossant, 1999), *Fgf8* (Crossley and Martin, 1995), *Gsc* (Blum et al., 1992), *Hesx1* (Thomas and Beddington, 1996), *Lefty1* and *Lefty2* (Meno et al., 1997), *Nodal* (Perea-Gomez et al., 2004) and *Wnt3* (Liu et al., 1999).

β-Galactosidase staining was carried out according to a standard protocol using 0.5 mg/ml X-gal (Fermentas). Embryos were embedded in Technovit 8100 (Heraeus Kulzer), sectioned and stained with 0.05% Neutral Red solution.

Immunohistochemistry with anti-E-cadherin (BD Transduction) and anti-Snail (Abcam) antibodies was performed using an automated platform (Ventana Discovery, Ventana Medical Systems) on 5 μm paraffin sections of 4% paraformaldehyde-fixed embryos.

Luciferase assay, treatment with siRNA, blockade of protein synthesis and western blotting

HEK293T cells were cultured in 96-well plates and transfected using Lipofectamine 2000 (Invitrogen). The following plasmids were used: Myc-tagged *Foxh1*, Flag-tagged *Cripto*, *Nodal* and *A3-luc* (Iratni et al., 2002); HA-tagged *Smad4* (de Winter et al., 1997); Flag-tagged *Smad1* and Flag-tagged *Smad5* (Imamura et al., 1997); and 3xFlag/Strep-tagged Smad5 and 3xFlag/Strep-tagged Δ-*Smad5* (F.C. and A.Z., unpublished). The latter is a Smad5 deletion mutant lacking the C-terminal SSXS domain. Recombinant human rhBMP4 50 ng/ml (R&D Systems) was used to stimulate cells. Cells were harvested after 24 hours for luciferase determination (Promega). Normalization was to β-galactosidase activity from co-transfected pCMVβ-gal plasmid (Clontech) assayed using Galscreen *Tropix* (Applied Biosystems). At least two independent experiments were performed in sextuplicates. Silencing endogenous *Smad5* was performed by co-transfecting ON-TARGET plus SMARTpool *Smad5* siRNA (Dharmacon) or non-targeting control siRNA at a final concentration of 10 nM. Blockade of protein synthesis was with cycloheximide 50 μg/ml (Merck) pretreatment of cells for 1 hour, followed by 5 hours stimulation with 50 ng/ml rhBMP4 in the presence of cycloheximide. RNA was extracted and purified (RNeasy RNA purification columns, Qiagen). Reverse transcription (RT) was with MuMLV reverse transcriptase (Revert-aid, Fermentas), oligo-dT_{18} and random primers (Invitrogen). *Luciferase* expression was analyzed by quantitative (q)RT-PCR, and normalized to β-galactosidase expression.

Western blot analysis was carried out according to standard procedures, using monoclonal M2 α-Flag (Sigma), α-Myc 9E10 (Santa Cruz) and α-

HA (CoVance), and polyclonal α-phosphoSmad1/5/8 (Cell Signaling), α-phosphoSmad5 or α-Smad5 (Epitomics), α-phosphoSmad2 (a gift from P. ten Dijke, LUMC, The Netherlands), α-Foxh1 (R&D), α-tubulin (ProBio) primary antibodies and HRP-conjugated secondary antibodies (Jackson ImmunoResearch). Chemiluminescence [ECL reagent (Perkin Elmer) or ECL advance (GE Healthcare Biosciences)] was detected with a LAS-3000 Imager (Fujifilm) and quantified with AIDA Image Analyzer V.4.2.2-software (Raytest).

Co-immunoprecipitation

HEK293T cells were cultured in 9 cm dishes and transfected as indicated using polyethyleneimine (PEI; Sigma), stimulated the next day with 25 ng/ml rhBMP4 for 8 hours, and lyzed using 170 mM NaCl, 10 mM EDTA, 50 mM NaF, 50 mM Tris-HCl (pH 7.4) and 0.5% Nonidet-P40 supplemented with 0.8 mM $Na_4P_2O_7.10H_2O$, 4 mM Na_3VO_4 and complete protease inhibitor (Roche). Lysates were incubated with the α-HA antibody overnight at 4°C, followed by precipitation of complexes with protein G Sepharose beads (GE Healthcare Biosciences) for 3 hours at 4°C. Beads were washed with lysis buffer and protein solubilization was in 2× SDS-containing sample buffer. Immunoprecipitates were analyzed by western blotting.

Endogenous Smad2-Smad5 interactions were demonstrated in human embryonic stem cells (H9) and MCF-7 cells. H9 cells were induced to undergo initial steps of mesendoderm/liver differentiation as described previously (Roelandt et al., 2010). At day 4 of differentiation, cells were stimulated with 50 ng/ml activin (R&D) or 50 ng/ml activin and 50 ng/ml rhBMP4 for 90 minutes. Serum-starved MCF-7 cells (DMEM 0.1% FCS) were transfected with ON-TARGET plus SMARTpools for *Smad5* and *Smad1* siRNA (Dharmacon) or non-targeting control siRNA (final concentration of 10 nM), and the following day they were ligand stimulated for 60 minutes.

Lysis of H9 or MCF-7 cells was with 100 mM KH_2PO_4, 0.2% Triton-X100, 1 mM DTT, 0.8 mM $Na_4P_2O_7.10H_2O$, 4 mM Na_3VO_4 and complete protease inhibitor (Roche). Sepharose G pre-cleared lysates were overnight incubated with anti-Smad2/3 antibody (R&D, AF3797) at 4°C, followed by precipitation of complexes as described for HEK293T cells.

Proximity ligation assay (PLA)

Serum-starved MCF-7 cells cultured on coverslips were stimulated with 100 ng/ml activin and 50 ng/ml rhBMP4 for 30 or 60 minutes and subjected to in situ PLA using Duolink Detection kit II (Olink Bioscience) using primary antibodies against Smad2 (Abcam, AB71109) and C-terminally phophorylated Smad1/5/8 (Cell Signaling, 9511S). Heteromers were counted in three fields per coverslip and three wells were analyzed per condition (Moya et al., 2012). Quantifications are given as mean±s.e.m. Statistical evaluation was carried out using Student's *t*-test ($P<0.05$ was considered significant; $^{***}P<0.001$).

Quantitative RT-PCR of amnion

Amnion samples from wild-type and *Smad5* knockout littermates were micro-dissected in ice-cold PBS at neural plate to headfold stages, followed by snap-freezing. Reverse transcription was performed in the sample lysate using SuperScript III Reverse Transcriptase (Invitrogen) and poly-dT universal primer 1. After 3′ poly-A tailing with terminal deoxynucleotidyl transferase (Invitrogen), second-strand cDNA was produced using poly-dT universal primer 2, followed by amplification consisting of 18 and 12 PCR cycles using poly-dT universal primers 1 and 2, and Ex Taq HS polymerase (Takara Bio) and column purification (QIAquick, QIAGEN). This procedure was adapted from double-stranded cDNA synthesis protocol from a single cell (Applied Biosystems demonstrated protocol). qPCR was performed in technical duplicates in 96-well plates using an ABI7000 instrument, each well containing 25 ng target cDNA, specific primer pair and Platinum SYBR Green qPCR SuperMix-UDG with ROX (Invitrogen). Primers (supplementary material Table S1) were in silico validated using RTPrimerDataBase (www.rtprimerdb.org). Relative RNA levels were calculated using the ΔΔCt method with *Gapdh* and *Ubc* as reference genes.

RESULTS

Formation of an ectopic primitive streak-like structure in *Smad5* mutant amnion

The development of an ectopic agglomerate of cells consistently located in the anterior midline quadrant of the amnion is a phenotype unique to $Smad5^{m1/m1}$ mutant mouse embryos. We hypothesized that the amniotic clump in *Smad5* mutants is an ectopic primitive streak-like structure. Analysis of the expression of several markers normally expressed in emerging mesoderm at the early primitive streak – brachyury (*T*), eomesodermin (*Eomes*), *Fgf8* and goosecoid (*Gsc*) – demonstrated that these markers were ectopically expressed in the clump in embryonic day (E) 8.5 *Smad5* mutants (Fig. 1A-D). Furthermore, analysis of mutant amnions at E7.5 by qRT-PCR demonstrated not only ectopic *T* and *Gsc* expression in most mutant amnions analyzed, but also ectopic expression of other primitive streak markers such as *Mixl1* and *Foxa2* (supplementary material Fig. S1A). This suggests that the clump of cells in the amnion of *Smad5* mutant embryos is an ectopic primitive streak-like structure.

In the primitive streak, epiblast cells ingress while undergoing EMT, a multi-pathway process associated with loss of E-cadherin and development of Snail-positive mesoderm (Tam and Loebel, 2007). To evaluate presence of ectopic EMT, we compared the localization of E-cadherin and Snail in amnion of *Smad5* mutant and control littermates. In wild-type amnion, E-cadherin localizes basolaterally in amniotic ectoderm shortly after amnion closure, whereas E-cadherin relocalizes mainly to the basal side of amniotic ectoderm when the ectoderm acquires its squamous architecture (supplementary material Fig. S1B,D). In contrast to the primitive streak region, Snail was not only detected in amniotic mesoderm but also in ectoderm of control amnion (supplementary material Fig. S1C,E, arrowheads). This observation concealed the analysis of (stereotype) EMT in the *Smad5* mutant amnion. Nonetheless, the staining for Snail appeared less uniform in the amniotic ectodermal side of the amniotic clump in *Smad5* mutant embryos (supplementary material Fig. S1D,F, outlined area). Such areas matched with regions of high E-cadherin in adjacent sections of the amniotic clump (supplementary material Fig. S1B,D). The amniotic mesodermal side of the clump facing the exocoelom was devoid of E-cadherin. Overall, the E-cadherin distribution seemed compatible with the amniotic clump in Smad5 mutant embryos, resembling an ectopic primitive streak-like structure.

Ectopic *Nodal* expression in *Smad5* mutant amnion

Expansion of the primitive streak or ectopic primitive streak formation is often associated with increased/ectopic *Nodal* expression and signaling. This has, for example, been demonstrated in compound mutants of the Nodal antagonists *Cer1* and *Lefty1*, which are normally secreted by the AVE (Perea-Gomez et al., 2002). Similarly, mice deficient in *Lefty2*, which is normally expressed in LPM at gastrula stages, develop an expanded primitive streak associated with increased Nodal signaling (Meno et al., 1999).

Nodal expression is undetectable in control amnion but *Nodal* mRNA becomes ectopically expressed in the amnion of $Smad5^{m1/m1}$ embryos from the neural plate (NP, E7.5) stage onwards, well before the first visible thickening of the *Smad5* mutant amnion (Fig. 2A). At the one-somite stage (1S, E8.0), ectopic *Nodal* was consistently observed in the anterior midline quadrant of the not yet thickened mutant amnion near the junction with anterior ectoderm (Fig. 2B), coinciding with where the amniotic clump would form. This suggests

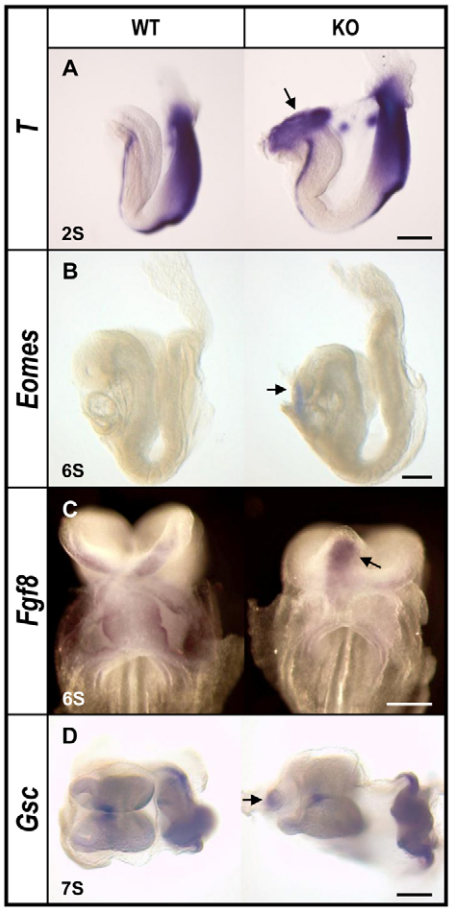

Fig. 1. Mesoderm markers expressed in primitive streak are ectopically expressed in the *Smad5* mutant amnion. (**A**) In situ hybridization for *T* in wild-type and *Smad5* knockout embryos at the two-somite (2S) stage. (**B**) *Eomes* in wild-type and *Smad5* knockout embryos at the 6S stage. (**C**) Frontal view of *Fgf8* in wild-type and *Smad5* knockout embryos at the 6S stage. (**D**) *Gsc* in wild-type and *Smad5* knockout embryos at 7S stage (top view). Arrows indicate the amniotic clump, including the ectopic expression of these mesoderm markers. Scale bars: 200 μm.

that ectopic *Nodal* presages the formation of the amniotic clump. Later, at the >5S stage (E8.5) when the amnion thickening is clearly discernible, ectopic *Nodal* remained detectable in the amniotic clump, in the left and right side of the cardiac crescent, and frequently in the distal tip of the allantois (5/7 embryos, Fig. 2C, supplementary material Fig. S2). These observations were confirmed by staining for β-galactosidase in *Smad5*-knockout embryos obtained after crossing $Smad5^{m1/+}$ heterozygotes with $Smad5^{m1/+}$;$Nodal^{lacZ/+}$ reporter mice (Fig. 2D,E). Reducing the allele dose of *Nodal* in these $Smad5^{m1/m1}$;$Nodal^{lacZ/+}$ embryos did not rescue the amnion defect (Fig. 2D,E). The three ectopic expression domains of *Nodal* in E7.5-E8.5 *Smad5* mutant embryos (Fig. 2A-C and supplementary material Fig. S2) overlapped with reported *Bmp2* (Ishimura et al., 2008; Madabhushi and Lacy, 2011) and *Bmp4* (Lawson et al., 1999) expression domains, and intense BMP/Smad activation in a BRE-*lacZ* reporter mouse (Monteiro et al., 2004) that monitors BMP/Smad1-5 signaling (Fig. 2F). These observations show that *Nodal* expression is regulated by BMP signaling in the amnion, but probably also in other regions of the embryo.

Chimeric embryos resulting from aggregation of $Smad5^{m1/m1}$ ES cells and diploid morulae still developed amniotic clumps despite the presence of wild-type visceral endoderm/AVE (Bosman et al., 2006). This demonstrates that the formation of a primitive streak-like structure in the amnion is not the indirect consequence of the absence of *Smad5* in AVE. Nonetheless, we analyzed the expression of mRNAs encoding the AVE secreted antagonists and also *Lefty2* in *Smad5* mutant embryos to determine whether the mechanisms that normally prevent *Nodal* expression and signaling in the anterior side of the embryo proper were affected. Analysis of the expression of *Cer1*, *Lefty1*, *Dkk1* and *Lefty2* revealed that their domains were similar in *Smad5* mutant and control littermates (Fig. 3A-D). Furthermore, comparable levels of expression of markers for most rostral ectoderm (*Dlx5*) and early forebrain (*Hesx1*) in *Smad5* mutant and control embryos, suggest that patterning of the anterior part of the embryo proper is preserved at this stage (Fig. 3E,F). This indicates that the known mechanisms of Nodal antagonism in the anterior side of the embryo are not affected in the *Smad5* mutants. Together, these data suggest the existence of a BMP/Smad5-dependent mechanism of regulation of *Nodal* expression in the amnion that prevents the formation of an ectopic primitive streak-like structure in this extra-embryonic tissue.

BMP/Smad5 signaling antagonizes the Nodal Smad2/Foxh1-dependent autoregulatory loop

Smad1-mediated BMP signaling was shown to affect *Nodal* expression in LPM by limiting the availability of Smad4 and a concomitant interference with the Nodal-Smad2/4-Foxh1-dependent autoregulatory loop (Furtado et al., 2008). To determine whether Smad5-mediated BMP signaling can antagonize the Nodal autoregulatory loop, we made use of a Nodal/Activin-responsive luciferase reporter, which contains Foxh1- and Smad2/4-binding sites from the *Mix2* promoter (Watanabe and Whitman, 1999). The effect of gain- and loss-of-function of Smad5-dependent BMP signaling was tested in these reporter assays. Notably, we used ligands to activate the signaling pathways, whereas others investigated the role of BMP/Smad1 signaling by using overexpression of constitutively active type I receptor/Alk variants (Furtado et al., 2008).

Using transfected HEK293T cells, co-production of Foxh1 and Cripto resulted in only mild activation of the reporter (Fig. 4A, lane 2), whereas co-synthesis of Nodal resulted in an ~12-fold increase in luciferase activity (Fig. 4A, lane 3). Stimulation with BMP4 for 5 or 20 hours progressively reduced the response to Nodal (Fig. 4A, lanes 4 and 5), an effect that has previously been reported (Osada et al., 2000). Repression of the reporter activity by BMP4 was further potentiated when Smad5 was co-produced (Fig. 4A, lanes 6 to 8). Transfection of a vector encoding a Smad5 mutant protein (Δ-Smad5) that can no longer be phosphorylated in its C-terminal SSXS domain, did not repress reporter activity (Fig. 4A, lanes 9 to 11). Furthermore, it tempered the phosphorylation of the endogenous Smad5, indicating that Δ-Smad5 probably functions as a dominant-negative Smad5 variant that interferes with the receptor-mediated activation of endogenous Smad5 (Fig. 4A). Similarly, silencing of endogenous *Smad5* by small interfering RNA (siRNA) potentiated Nodal signaling (Fig. 4B, lane 6). Synthesis of exogenous mouse Smad5 in siRNA-treated cells restored the inhibitory effect of Smad5 on Nodal signaling (Fig. 4B, lanes 7 and 8). These results demonstrated that activated Smad5 signaling tempers Nodal signaling, and that C-terminal activation of Smad5 is essential to repress Nodal signaling.

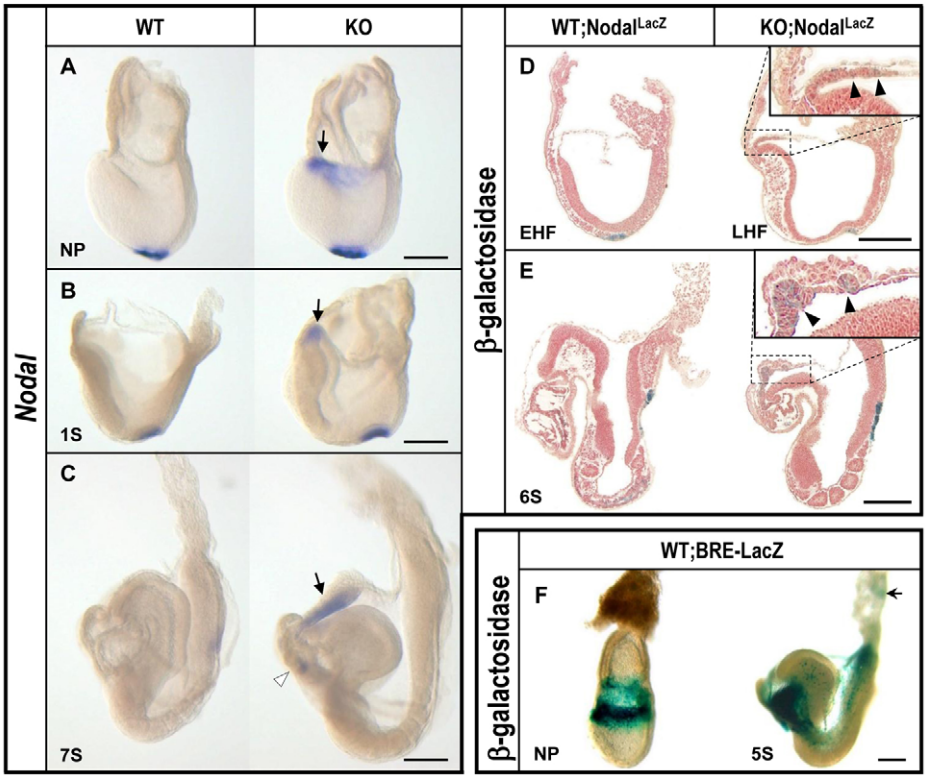

Fig. 2. Ectopic *Nodal* mRNA expression in *Smad5* mutants coincides with regions of intense BMP/Smad signaling in wild types. (**A-C**) *Nodal* expression in wild-type and *Smad5* knockout embryos at (A) neural plate (NP), (B) 1S and (C) 7S stages. Ectopic *Nodal* in amnion (arrow) and cardiac crescent (arrowhead in C). (**D**,**E**) β-Galactosidase staining of *Smad5* knockout and control littermates from $Smad5^{m1/+} \times Smad5^{m1/+};Nodal^{lacZ/+}$ crosses at (D) headfold and (E) 6S stages. Insets in knockout panels are magnifications of boxed areas. Arrowheads indicate the ectopic *Nodal* and the peculiar cellular architecture of amniotic ectoderm. (**F**) Staining for β-galactosidase in *BRE-lacZ* embryos reporting BMP/Smad signaling at NP and 5S stages. The arrow indicates BMP-Smad signaling in the distal tip of the allantois. Scale bars: 200 μm.

Interestingly, activation by the liganded Nodal receptor complex seemed undisturbed by BMP signaling because high levels of phospho-Smad2 were maintained under all conditions where Nodal was present, regardless of stimulation with BMP (Fig. 4A). This excludes the possibility that BMP/Smad5 signaling is upstream of the expression of secreted Nodal antagonists or interferes with activation of the Nodal receptor complex. Activated Smad5 may limit the availability of Smad4 to activated Smad2, as proposed previously for BMP/Smad1 signaling during establishment of LR asymmetry [see above (Furtado et al., 2008)]. However, in our experimental setup, stimulation with ligand at increasing doses of co-transfected Smad4 did not restore the BMP4-mediated repression on the response to Nodal (Fig. 4C). This indicated that, in this case, Smad5 does not limit the availability of Smad4 to Smad2 upon activation of the latter by Nodal.

Next, we examined the effect of increasing quantities of Smad5 or Smad1 in the luciferase assay in the presence of exogenous Smad4. Activated Smad1 and Smad5 inhibited Nodal signaling in a dose-dependent manner (Fig. 4D). The lower decrease in Nodal signaling with Smad1, when compared with Smad5, correlated with the lower phosphorylation status of Smad1 (Fig. 4D, considering the ratio of phospho-Smad1/5/8 over tubulin in the α-phospho-Smad1/5/8 and α-tubulin blots). This suggests that activated Smad1 and Smad5 have similar potential to antagonize Nodal signaling in vitro.

Blocking protein translation with cycloheximide prior to stimulation with BMP4 (supplementary material Fig. S3) did not affect repression of *Nodal*-dependent luciferase expression by activated BMP/Smad5 (Fig. 5A, lane 6). In our experimental setup, Nodal signaling is therefore directly regulated by BMP/Smad5 signaling.

Endogenous Smad5-Smad2 interactions

The persistence of high phospho-Smad2 levels in the reporter assays (Fig. 4A) suggested that Smad5 interferes downstream of Nodal receptor and Smad2 activation. Furthermore, we found that Smad5 did not influence Nodal signaling by limiting the availability of Smad4. We therefore investigated whether activated Smad5 co-immunoprecipitated with Smad2 and whether this interaction would affect co-precipitation of Foxh1 with Smad2. HA-tagged Smad2 was immunoprecipitated from whole-cell extracts of HEK293T cells producing HA-tagged Smad2, Myc-tagged Foxh1 and 3xFlag/Strep-tagged Smad5 or 3xFlag/Strep-tagged Δ-Smad5 in the presence or absence of BMP. Foxh1 co-immunoprecipitated with Smad2 when Nodal signaling was active (Fig. 5B, lanes 3 and 7, panel HA-Smad2 IP). Smad5 co-precipitated with Smad2; however, upon stimulation with BMP4, co-immunoprecipitation of Smad5 – but not Δ-Smad5 – with Smad2 was enhanced (Fig. 5B, lanes 4 and 8, respectively). This is consistent with the reporter assays, where phosphorylation of Smad5 was found to be required to decrease Nodal signaling. Furthermore, BMP4/Smad5 signaling negatively impacted on the co-immunoprecipitation of Foxh1 with Smad2 (Fig. 5B, lane 4). The condition with BMP4/Δ-Smad5 seems also to reduce co-immunoprecipitation of Foxh1 with Smad2 (Fig. 5B, lane 8), which can be explained by remaining activation of endogenous Smad1/5 in HEK293T cells. These data indicate that activation of the BMP pathway resulted in interaction of Smad5 with Smad2, which in turn interfered with Smad2-Foxh1 complex formation.

Subsequently, endogenous Smad5-Smad2 interactions were detected in human H9 embryonic stem cells (ESCs) and breast cancer MCF-7 cells. To obtain H9 cells that were fully BMP4 and activin responsive, cells were differentiated towards mesendoderm using a liver differentiation protocol (Roelandt et al., 2010). On day 4 of the differentiation, cells were co-stimulated with activin and BMP4, or with activin alone for 90 minutes. Smad2/3 was immunoprecipitated from whole-cell extracts. Co-immunoprecipitation of (phospho)Smad5 with Smad2/3 was observed when cells were co-stimulated with BMP4 and activin (Fig. 5C).

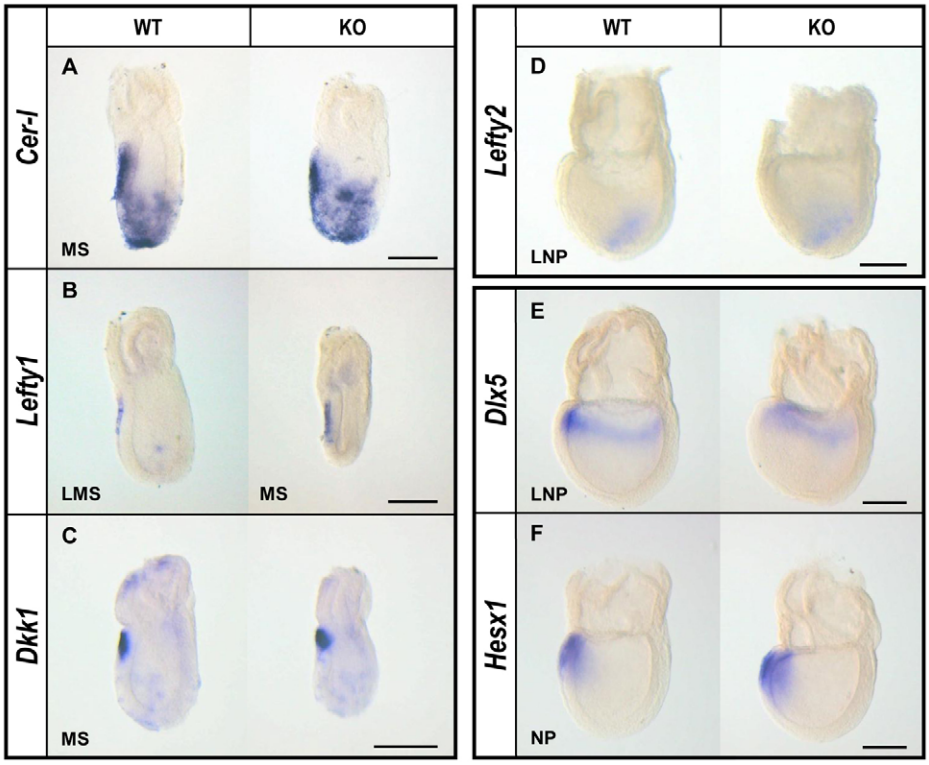

Fig. 3. AVE is established and functional, and expression of *Lefty2* in LPM is not affected in Smad5 mutants. (**A-C**) In situ hybridization for *Cer1* (A), *Lefty1* (B) and *Dkk1* (C) in wild-type and *Smad5* knockout embryos at mid-streak (MS) stage. (**D**) *Lefty2* in wild-type and *Smad5* knockout embryos at late neural plate (LNP) stage. (**E**,**F**) Expression of early forebrain markers *Dlx5* (E) and *Hesx1* (F) in wild-type and *Smad5* knockout embryos at LNP (E) and NP (F) stages. Scale bars: 200 μm.

Endogenous ligand-induced Smad5-Smad2 interactions were also demonstrated in MCF-7 cells (Yum et al., 2009), and the reduced presence of such complexes in MCF-7 cells upon siRNA mediated knock-down of Smad5 and Smad1 further demonstrated the specificity of the Smad5-Smad2 complexes (Fig. 5D). The impact of Smad5-Smad2 complex formation on Smad2-Foxh1 heteromerization was – in contrast to the observations in overexpression (Fig. 5B) – marginal in H9 and MCF7 cells. In addition to the endogenous co-immunoprecipitation experiments, Smad5 and Smad2 interactions were also visualized and quantified by in situ proximity ligation assay (PLA) (Fig. 5E). The co-stimulation with activin and BMP4 resulted in a threefold increase in the number of Smad5-Smad2 heteromers when compared with basal levels (Fig. 5E).

The Nodal autoregulatory loop induces ectopic *Nodal* in the *Smad5* mutant amnion

The lack of effective tools to detect endogenous Smad5-Smad2 interactions in the mouse embryo prohibited analyzing whether Nodal and BMP/Smad5-mediated signaling results in direct Smad5-Smad2 interaction in the amnion, which would support the BMP/Smad5-mediated antagonism of the Nodal autoregulatory loop in vivo. Therefore, we performed a comparative gene expression analysis on RNA isolated from individual amnions of *Smad5* mutant and control littermates from neural plate until headfold stages, well before morphological appearance of the cell clump in mutant amnion, and tested the expression of *Nodal* and *Lefty2* as target genes of the Nodal autoregulatory loop. In addition, the expression of *Nodal*, *Bmp4* and *Wnt3* was used as read-out of activation of the slow positive feedback loop.

Ectopic *Nodal* was detected in most of the *Smad5* mutant amnions analyzed (20/26) (Fig. 6A). Ectopic *Lefty2* was also detected in the majority of the mutant amnions but in fewer embryos than *Nodal* (15/26). In situ hybridization analysis demonstrated ectopic *Lefty2* in the amniotic clump, in allantois and both sides of the cardiac crescent at E8.5 (Fig. 6C), which correlated with ectopic *Nodal* at a similar stage (Fig. 2C, supplementary material Fig. S1). Altogether, these results support the involvement of Smad2/4-Foxh1 signaling in the mutant amnion and are compatible with Nodal autoregulatory loop activity.

None of the amnions analyzed here showed differential *Bmp4* expression (Fig. 6A), which contrasted to increased *Bmp4* in *Smad5* mutant amnion at E7.5 that was detected by radioactive in situ hybridization (Bosman et al., 2006). Unlike the unchanged *Bmp4* levels, *Wnt3* expression is ectopically expressed in nearly half of the *Smad5* mutant amnions analyzed by RT-PCR (12/26) (Fig. 6A). Indeed, in situ hybridization analysis confirmed ectopic *Wnt3* in the mutant amnion at headfold stages and demonstrated that it persisted in the amnion thickening at E8.5 (Fig. 6D,E). Furthermore, crossing of the $Smad5^{m1/+}$ with the Lef/Tcf-dependent Wnt signaling reporter mouse ($Smad5^{m1/+}$;$BAT\text{-}gal^{+/-}$) showed that ectopic canonical Wnt signaling occurred in *Smad5*-deficient amnion (Fig. 6F-H). Taking into consideration that canonical Wnt3 signaling induces *Nodal* via an identified proximal epiblast enhancer (PEE) in its promoter containing Lef/Tcf-binding sites (Ben-Haim et al., 2006; Granier et al., 2011), our data are also in agreement with the presence of a functional slow positive-feedback loop in *Smad5* mutant amnion.

The higher prevalence of amnions expressing ectopically target genes from the Nodal-Smad2/4-Foxh1-dependent feedback loop, namely *Nodal* and *Lefty2*, rather than *Wnt3* (slow positive-feedback loop component), is compatible with induction of ectopic *Nodal* by the fast autoregulatory loop in the *Smad5* mutant amnion. This became more evident when *Smad5* mutant amnions were divided into classes according to their ectopic expression profile (Fig. 6B). Three of the $Smad5^{m1/m1}$ amnions had no ectopic expression of any of these genes, suggesting that the defect had not been initiated in these embryos at the time of amnion isolation. Three mutant

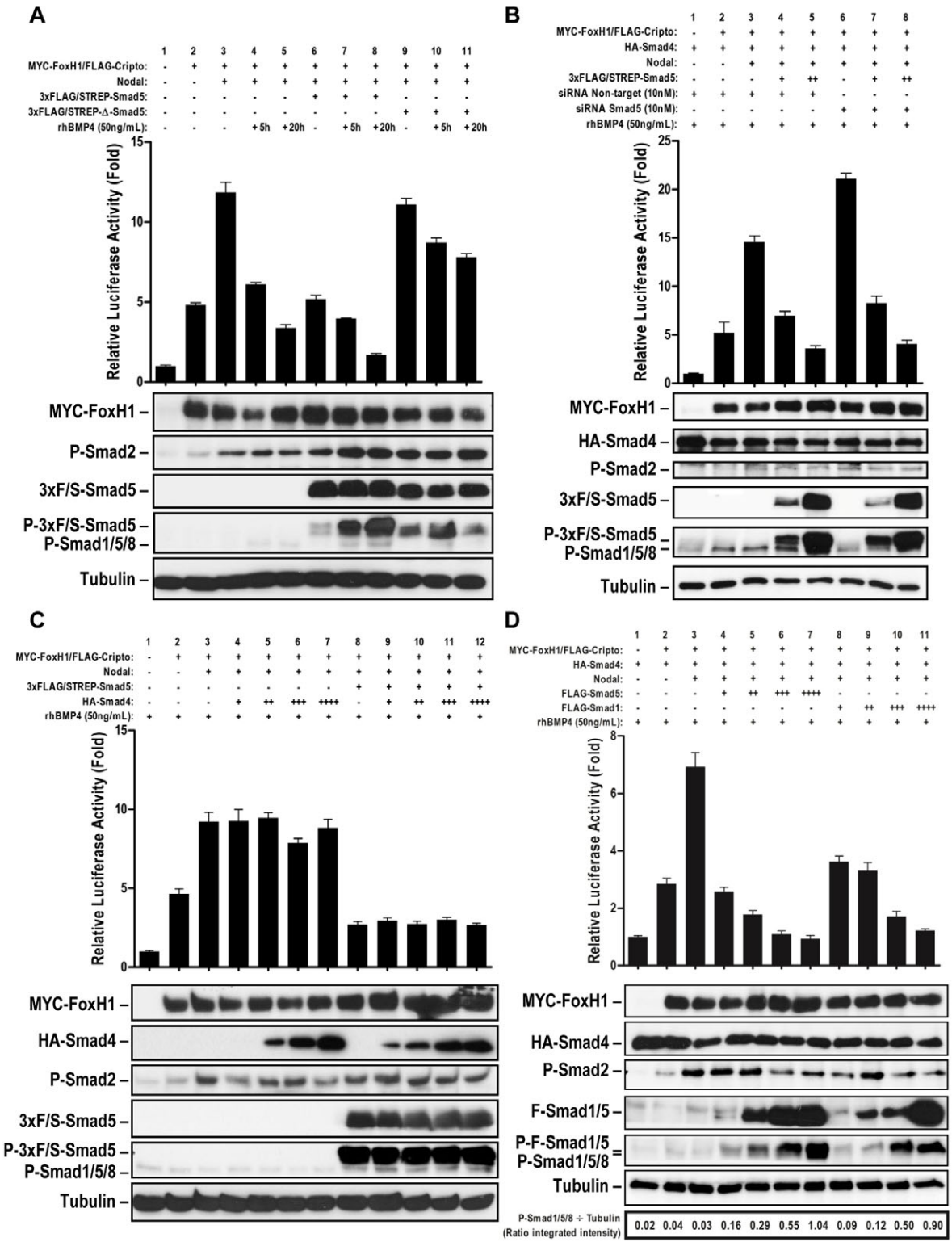

Fig. 4. BMP/Smad5 signaling decreases Nodal signaling. (**A**) BMP4/Smad5 signaling decreases Nodal signaling activity. Nodal signaling was assayed by using the Nodal/Activin responsive *A3-luc* reporter in HEK293T cells co-transfected with expression constructs for *Nodal*, Flag-tagged *Cripto*, Myc-tagged *Foxh1* and β-galactosidase in the presence or absence of 3xFlag/Strep-tagged (3xFS) *Smad5* or 3xFlag/Strep-tagged *Δ-Smad5*. BMP stimulation was as indicated for 20 hours. (**B**) Knockdown of *Smad5* enhanced Nodal signaling, and co-transfection with mouse 3xFlag/Strep-tagged *Smad5* rescued the decrease of Nodal signaling. HA-tagged *Smad4* was transfected additionally and cells were stimulated with 50 ng/ml rhBMP4. (**C**) The effect of BMP4/Smad5 signaling on Nodal signaling does not depend on Smad4 levels. (**D**) Activated Smad1 and Smad5 are similarly competent to decrease Nodal signaling activity. The lower panels in A-D show expression analysis of the respective expression constructs and the phosphorylation status of Smad2 and Smad1/5/8 by western blotting. Tubulin was used as a control. The ratio of phospho-Smad1/5/8 to tubulin represents the activation status of transfected Smad1 or Smad5 per condition. Data are mean±s.d.

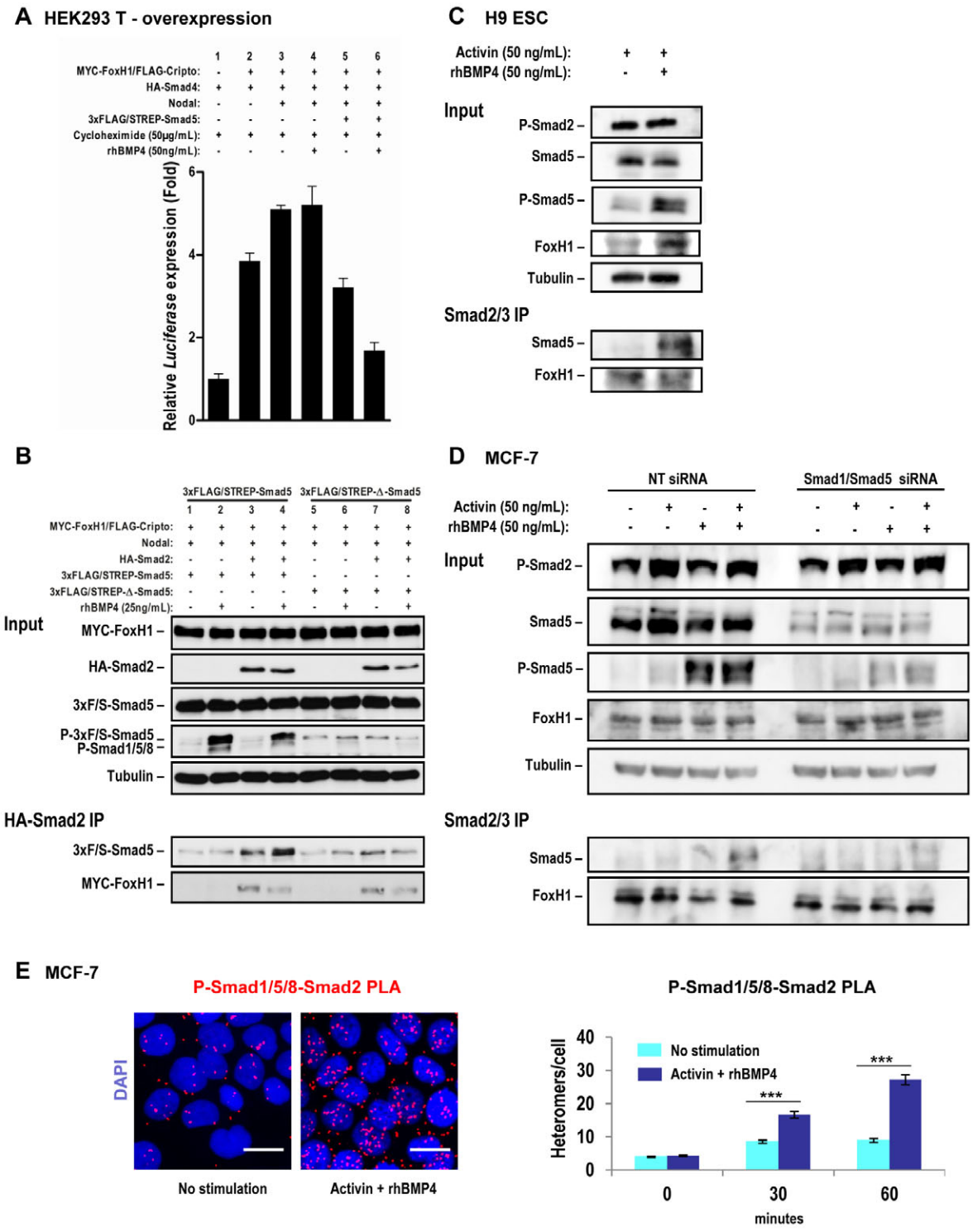

Fig. 5. Smad5 directly affects Nodal signaling through BMP-induced interaction of Smad5 with Smad2. (**A**) The effect of Smad5 on Nodal signaling does not require target gene expression. Nodal signaling was quantified by qRT-PCR expression analysis of *luciferase* driven by the Nodal/activin responsive *A3-luc* reporter in HEK293T cells. Cells are co-transfected with expression constructs for *Nodal*, Flag-tagged *Cripto*, Myc-tagged *Foxh1* and β-galactosidase in the presence or absence of 3xFlag/Strep-tagged *Smad5*. Cells were pre-treated with 50 μg/ml cycloheximide for inhibition of protein synthesis (supplementary material Fig. S3). Transfected cells were stimulated with 25 ng/ml rhBMP4 for 8 hours as indicated. (**B**) Smad5 is specifically co-immunoprecipitated with HA-tagged Smad2 upon rhBMP4 stimulation of HEK293T cells co-transfected with constructs for *Nodal*, Flag-tagged *Cripto*, Myc-tagged *Foxh1* and 3xFlag/Strep-tagged *Smad5* or 3xFlag/Strep-tagged *Δ-Smad5* in the presence or absence of HA-tagged *Smad2*. (**C**) Endogenous interaction between Smad5 and Smad2/3 is revealed by co-immunoprecipitation using H9 cells; cells were stimulated for 90 minutes. (**D**) Endogenous Smad5 is specifically co-immunoprecipitated with Smad2/3 from MCF-7 cells when cells are stimulated with rhBMP4 and activin for 60 minutes. (**E**) Phospho-Smad1/5/8-Smad2 heteromers detected by in situ PLA using α-phospho-Smad1/5/8 and α-Smad2 antibodies (left), and PLA signal quantification (right). Scale bars: 20 μm. Data are mean±s.d. (A) and mean±s.e.m. (E).

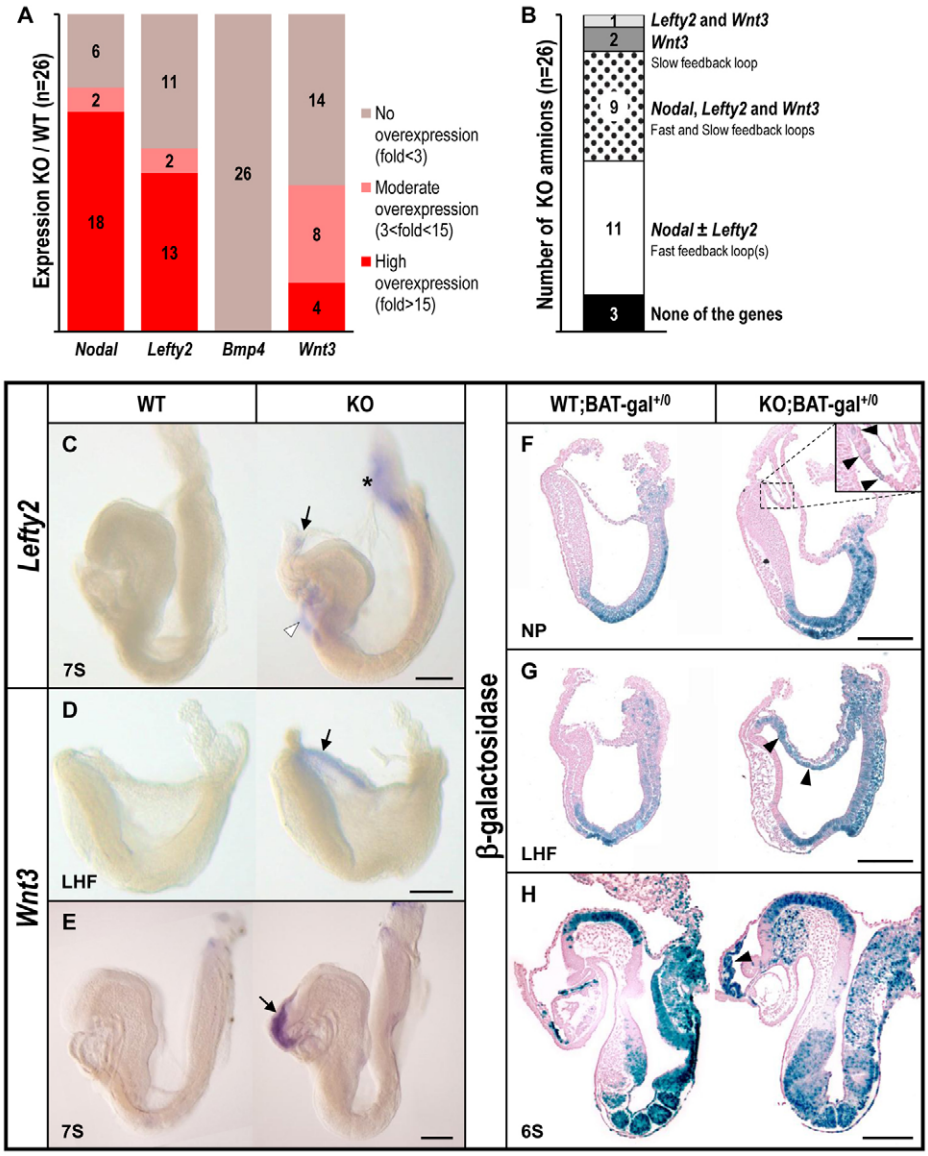

Fig. 6. Active Nodal feedback loops in the *Smad5* mutant amnion. (**A**) Analysis of *Nodal*, *Lefty2*, *Bmp4* and *Wnt3* in *Smad5* knockouts compared with control littermate amnions by qRT-PCR (n=26 amnion pairs). (**B**) Categorization of *Smad5* mutant amnions according to their ectopic expression profiles. (**C**) In situ hybridization of *Lefty2* in wild-type and *Smad5* knockout embryos at 7S stage reveals ectopic *Lefty2* in the *Smad5* mutant amnion (arrow), heart (arrowheads) and allantois (asterisk) (**D**,**E**) *Wnt3* expression in wild-type and *Smad5* knockout embryos at (D) late headfold (LHF) stage and (E) 7S stage. Arrows indicate ectopic *Wnt3* in mutant amnion. (**F-H**) β-Galactosidase staining of $Smad5^{m1/+} \times Smad5^{m1/+}$;*BAT-gal* embryos at (F) NP stage, (G) late headfold (LHF) stage and (H) 6S stage. Insets are magnifications of boxed areas. Arrowheads show that ectopic canonical Lef/Tcf-dependent Wnt signaling is predominant in amniotic ectoderm. Scale bars: 200 μm.

amnions were found to express only *Wnt3* ectopically, or both *Wnt3* and *Lefty2* ectopic expression but not *Nodal*. During dissection, our efforts to prevent contamination of amnion samples with non-amnion tissue may have resulted in 3/26 samples in loss of the ectopic *Nodal* expression domain, which is typically restricted to the anterior most part of the amnion. From all the *Smad5* mutant amnions with ectopic *Nodal* expression, 11 expressed only Nodal-Smad2/4-Foxh1-dependent target genes (*Nodal* ± *Lefty2*), suggesting that ectopic *Nodal* in the *Smad5* mutant amnion is induced via the Smad2/Foxh1-dependent autoregulatory loop. The remaining nine mutant amnions co-expressed *Wnt3* (Fig. 6B), suggesting that the slow positive-feedback loop contributes to the amplification of ectopic *Nodal* in the mutant amnion. This observation, however, does not exclude the possibility that both loops initiate simultaneously in the *Smad5* mutant amnion, but as the slow positive-feedback loop requires the expression and signaling of the effector proteins, it probably takes longer to have an effect on *Nodal* expression. In conclusion, these data support that, in the absence of Smad5, the ectopic *Nodal* in the mutant amnion is induced by the Nodal autoregulatory loop and is amplified via the slow positive-feedback loop.

DISCUSSION

The lack of Smad5 in mouse embryos results in ectopic *Nodal* expression and signaling in the anterior part of the amnion, leading ultimately to the formation of an ectopic primitive streak-like structure therein. Before appearance of the clump in the *Smad5* mutant amnion, ectopic *Nodal* localizes in cuboidal amniotic ectoderm at the anterior midline quadrant of the amnion, whereas the remainder of the mutant amniotic ectoderm acquires the characteristic squamous amniotic epithelium architecture. The (1) altered cellular architecture of the amniotic ectoderm in the anterior midline quadrant of the mutant amnion, (2) the ectopic presence of mesoderm inducers herein, (3) the subsequent presence of several mesoderm markers, including *Eomes* (which is required in the primitive streak region to downregulate E-cadherin and allow EMT) (Arnold et al., 2008), and (4) the altered regionalized localization of E-cadherin and Snail are compatible with the amniotic clump in the Smad5 mutant embryo being an ectopic primitive streak-like structure.

Development of (multiple) ectopic primitive streak(s) in the epiblast has been described in *Cer-l;Lefty1* compound mutants (Perea-Gomez et al., 2002). Analysis of AVE secreted antagonists

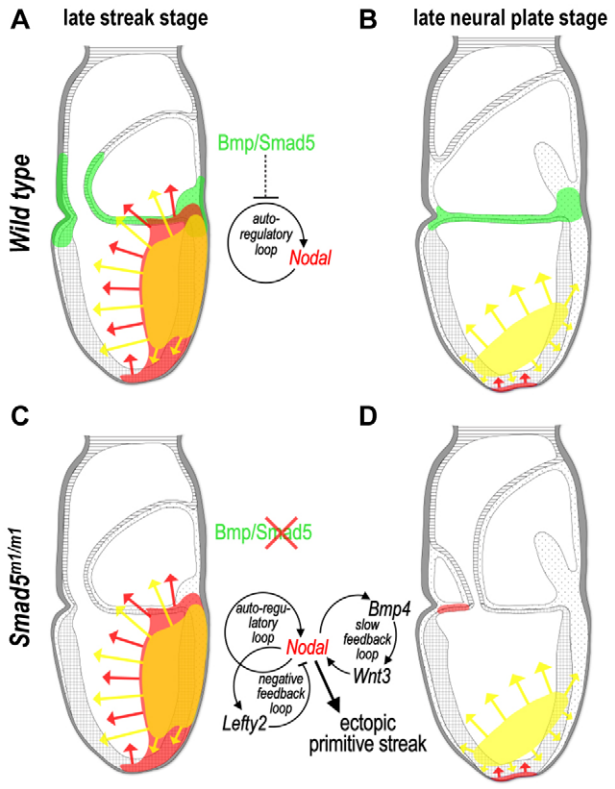

Fig. 7. Antagonism of Nodal signaling by BMP/Smad5 signaling in amnion. (**A**,**B**) BMP/Smad5 signaling (green) and Lefty2 (yellow) antagonize the Nodal-Smad2/4-Foxh1-dependent autoregulatory loop, restricting *Nodal* expression (red) to the node and resulting in normal amnion fate in wild-type embryos at E7.5. (**C**,**D**) Conversely, induction of *Nodal* expression by the Nodal autoregulatory loop and amplification via the slow positive-feedback loop culminate in ectopic *Nodal* and formation of an ectopic primitive streak-like structure in the Smad5-deficient amnion.

and neural plate/early forebrain markers (Thomas and Beddington, 1996) demonstrated that the *Smad5* mutant AVE is well established, maintained and functional. These data complement our former analysis of chimeric embryos that developed amniotic clumps even when AVE/visceral endoderm lineages were derived from wild-type recipient embryos (Bosman et al., 2006), suggesting that ectopic *Nodal* is not associated with an impaired AVE.

Ectopic expression of *T* has been shown in amnion of *Lefty2*-deficient embryos (Meno et al., 1999) and, hence, we reasoned that Lefty2 may diffuse from the nascent mesoderm and antagonize Nodal signaling in amnion. However, the expression of *Lefty2* in LPM appeared unaffected in *Smad5* mutants at late NP stage. Collectively, these data suggest that BMP/Smad5-mediated signaling antagonizes Nodal signaling in the amnion, preventing the propagation of *Nodal*-regulating loops that may ultimately lead to formation of ectopic primitive streak-like structures.

Removal of one allele of *Nodal* in a *Smad5* mutant background (*Smad5*$^{m1/m1}$;*Nodal*$^{lacZ/+}$) did not rescue the amnion phenotype or the different ectopic *Nodal* expression domains. This contrasts with the partial rescues reported when crossing this same *Nodal*^{lacZ} mouse strain with various other loss-of-function mice with increased *Nodal* and concomitant enforced mesoderm formation, including mutants of the AVE-secreted Nodal antagonists, and of *Drap1*, *Lefty2* and *Cyp26* (Iratni et al., 2002; Meno et al., 1999; Perea-Gomez et al., 2002; Uehara et al., 2009). The rescue of the *Lefty2* mutants by *Nodal* haploinsufficiency is, however, only modest. The lateral expansion of the expression domain of mesoderm markers expressed early during primitive streak formation was maintained in *Lefty2* mutants, but ectopic expression of these same marker genes in more anterior regions or even the amnion was lost (Meno et al., 1999). So, reducing the Nodal signaling levels by (about) half in the amnion seems sufficient to block defects caused by the absence of *Lefty2*. These findings are consistent with the existence of a BMP/Smad5-mediated mechanism that contributes normally to neutralize Nodal signaling in the amnion at E7.5.

Our data show that BMP-dependent antagonism of the Nodal autoregulatory loop is not restricted to Smad1 (Furtado et al., 2008). Indeed, BMP/Smad5 attenuates Smad2/4-Foxh1-mediated Nodal signaling in cultured cells; interfering with BMP/Smad5 activity, either by siRNA-mediated silencing of endogenous *Smad5* or by co-synthesis of a dominant-negative Smad5 variant, results, respectively, in increased or sustained high levels of Nodal signaling. Conversely, stimulation with BMP and activation of endogeneous Smad5 results in decreased Nodal signaling. Activated Smad5 directly regulates Nodal signaling downstream of Smad2 phosphorylation. Mixed activated Smad complexes between the BMP-Smads and TGFβ/Activin/Nodal-Smads in response to stimulation of epithelial cells with TGFβ have previously been reported (Daly et al., 2008; Gronroos et al., 2012). According to the present co-immunoprecipitation data on overexpression, co-activation of BMP and Nodal/Activin pathways induces the formation of Smad5-Smad2 complexes; in addition, such complexes are also demonstrated to occur endogenously in two different cell lines by two independent methods. We demonstrate that these complexes result in reduced Smad2-Foxh1 interaction and a concomitant reduced signaling via the Nodal Smad2/4-Foxh1-dependent autoregulatory loop in overexpression conditions.

Considering that we are technically unable to determine in the mouse embryo whether antagonism of the Nodal autoregulatory loop by BMP/Smad5 in the amnion requires Smad2-Smad5 heteromerization, the possibility remains that BMP/Smad5 affects Nodal signaling by competing for Smad4, as has been proposed for BMP/Smad1 (Furtado et al., 2008). Alternatively, BMP/Smad5 may compete for other shared transcription factors or adapter proteins and/or antagonize Nodal signaling indirectly [e.g. Jmjd3 (Kdm6b – Mouse Genome Informatics) (Dahle et al., 2010), Cited2 (Lopes Floro et al., 2011) and Xmsx-1 (Yamamoto et al., 2001b)]. Regardless of the mechanism, our data indicate that BMP/Smad5 signaling is required, in addition to Lefty2 (Meno et al., 1999), to antagonize Nodal signaling in amnion (Fig. 7A). Lefty2 that is induced in LPM by Nodal signaling has higher diffusion properties than Nodal ligand itself (Sakuma et al., 2002) and may therefore restrict Nodal signaling efficiently in the majority of the epiblast at E7.5, including in the amnion. As a consequence, *Nodal* expression becomes confined to the node region and the amnion acquires its typical squamous architecture (Fig. 7B). In the *Smad5* mutants, minute availability of Nodal signaling in anterior *Smad5*-deficient amnion can be expected to lead to ectopic *Nodal* induced via the Nodal-Smad2/Foxh1-dependent autoregulatory loop and is amplified by the slow positive-feedback loop (Fig. 7C,D). The signaling by the major primitive streak inducers in *Smad5* mutant amnion leads to ectopic primitive streak-like formation. This mechanism is probably more important in the anterior midline

quadrant of the amnion, which is the most distant from the source of Lefty2, where the primitive streak-like structure forms in the *Smad5* mutant. Alternatively, the focal localization of this structure may reflect the different properties and origin of the (mutant) anterior amniotic ectoderm cells that are localized at the anterior delineation between neural, surface and amnion ectoderm at the extra-embryonic/embryonic junction. Furthermore, *Bmp2* expression has recently been demonstrated in visceral endoderm close to the anterior extra-embryonic/embryonic junction, coordinating morphogenetic cell behaviors in multiple epiblast-derived lineages (Madabhushi and Lacy, 2011). The *Bmp2*- and *Smad5*-null mice both display anterior amnion morphogenesis defects (Chang et al., 1999; Zhang and Bradley, 1996) and hence it is plausible that impaired BMP2/Smad5-mediated signaling underlies the focal localization of the primitive streak-like structure in Smad5 mutant amnion.

Interestingly, *Nodal* is also ectopically expressed in the Smad5 mutant distal allantois and cardiac crescent, which are also regions undergoing active BMP/Smad signaling, as revealed in BRE-*lacZ* embryos. This suggests that an interplay between Nodal and BMP/Smad(5) signaling may also occur in other sites where Nodal and BMP co-signal. The distal allantois and cardiac crescent may, however, have lost competence to primitive streak-inducing signals at E8.0.

Detection of ectopic *Lefty2* by qRT-PCR shortly after the onset of ectopic *Nodal* in the *Smad5*-deficient amnion indicates that the Smad2-Foxh1-dependent negative-feedback loop is also activated in the mutant amnion. This may explain why mutant amniotic mesoderm becomes progressively patterned into more BMP-dependent posterior primitive streak derivatives at E8.5 (Bosman et al., 2006). Previously, we reported that gain-of-function of BMP signaling by injection rhBMP4 into the amniotic cavity of wild-type embryos could partially phenocopy the initial phase of amniotic clump formation (Bosman et al., 2006). Small rudimentary amnion thickenings were observed in a fraction of the injected embryos. Although gene expression analysis was not performed, histomorphological analysis was not indicative of ectopic primitive streak formation and mesoderm patterning. Injected BMP4 alone is probably insufficient to induce formation of ectopic primitive streak-like structures in amnion.

It is remarkable that *Smad5* mutant amnion is still competent for primitive streak induction at E7.5. This may reflect the fairly naïve state of the amnion at that stage, which could even persist until later stages. Indeed, human and rodent term amnion were recently described to harbor resident stem cell-like cells (Dobreva et al., 2010); whether such cells are functional stem cells retaining the potential to contribute to amnion homeostasis is unclear. Here, we provide evidence that BMP/Smad5 signaling is a pivotal regulator of early amnion fate through insulation of the amnion from Nodal signaling.

Acknowledgements
We thank all Zwijsen/Huylebroeck team-members: K. Beets, S. Thysen, P. Hembrechts and L. Ordovas for assistance; M. Missoul for mouse husbandry; S. Piccolo, J. Collignon, R. Monteiro and C. Mummery for reporter mice; J. Debruyn and M. Chen for probe/plasmids; P. ten Dijke for anti-phospho-Smad2 antiserum; and K. A. Lawson for instructive discussions.

Funding
P.N.G.P. was a predoctoral fellow of Fundação para a Ciência e Tecnologia (FCT) [SFRH/BD/15901/2005] (GABBA program class of 2005). This work was supported by FCT; Interuniversity Attraction Poles Program IUAP-6; and FWO-V (G.0382.07), OT-09/053 and GOA-11/012 from the KU Leuven Research Council. M.P.D. and I.M.M. were VIB11 predoctoral fellows.

Competing interests statement
The authors declare no competing financial interests.

Supplementary material
Supplementary material available online at
http://dev.biologists.org/lookup/suppl/doi:10.1242/dev.075465/-/DC1

References

Arnold, S. J., Maretto, S., Islam, A., Bikoff, E. K. and Robertson, E. J. (2006). Dose-dependent Smad1, Smad5 and Smad8 signaling in the early mouse embryo. *Dev. Biol.* **296**, 104-118.
Arnold, S. J., Hofmann, U. K., Bikoff, E. K. and Robertson, E. J. (2008). Pivotal roles for eomesodermin during axis formation, epithelium-to-mesenchyme transition and endoderm specification in the mouse. *Development* **135**, 501-511.
Bachiller, D., Klingensmith, J., Kemp, C., Belo, J. A., Anderson, R. M., May, S. R., McMahon, J. A., McMahon, A. P., Harland, R. M., Rossant, J. et al. (2000). The organizer factors Chordin and Noggin are required for mouse forebrain development. *Nature* **403**, 658-661.
Belo, J. A., Bouwmeester, T., Leyns, L., Kertesz, N., Gallo, M., Follettie, M. and De Robertis, E. M. (1997). Cerberus-like is a secreted factor with neutralizing activity expressed in the anterior primitive endoderm of the mouse gastrula. *Mech. Dev.* **68**, 45-57.
Ben-Haim, N., Lu, C., Guzman-Ayala, M., Pescatore, L., Mesnard, D., Bischofberger, M., Naef, F., Robertson, E. J. and Constam, D. B. (2006). The nodal precursor acting via activin receptors induces mesoderm by maintaining a source of its convertases and BMP4. *Dev. Cell* **11**, 313-323.
Blum, M., Gaunt, S. J., Cho, K. W., Steinbeisser, H., Blumberg, B., Bittner, D. and De Robertis, E. M. (1992). Gastrulation in the mouse: the role of the homeobox gene goosecoid. *Cell* **69**, 1097-1106.
Bosman, E. A., Lawson, K. A., Debruyn, J., Beek, L., Francis, A., Schoonjans, L., Huylebroeck, D. and Zwijsen, A. (2006). Smad5 determines murine amnion fate through the control of bone morphogenetic protein expression and signalling levels. *Development* **133**, 3399-3409.
Chang, H., Huylebroeck, D., Verschueren, K., Guo, Q., Matzuk, M. M. and Zwijsen, A. (1999). Smad5 knockout mice die at mid-gestation due to multiple embryonic and extraembryonic defects. *Development* **126**, 1631-1642.
Chang, H., Zwijsen, A., Vogel, H., Huylebroeck, D. and Matzuk, M. M. (2000). Smad5 is essential for left-right asymmetry in mice. *Dev. Biol.* **219**, 71-78.
Chen, C. and Shen, M. M. (2004). Two modes by which Lefty proteins inhibit nodal signaling. *Curr. Biol.* **14**, 618-624.
Cheng, S. K., Olale, F., Brivanlou, A. H. and Schier, A. F. (2004). Lefty blocks a subset of TGFbeta signals by antagonizing EGF-CFC coreceptors. *PLoS Biol.* **2**, E30.
Chocron, S., Verhoeven, M. C., Rentzsch, F., Hammerschmidt, M. and Bakkers, J. (2007). Zebrafish Bmp4 regulates left-right asymmetry at two distinct developmental time points. *Dev. Biol.* **305**, 577-588.
Ciruna, B. G. and Rossant, J. (1999). Expression of the T-box gene Eomesodermin during early mouse development. *Mech. Dev.* **81**, 199-203.
Crossley, P. H. and Martin, G. R. (1995). The mouse Fgf8 gene encodes a family of polypeptides and is expressed in regions that direct outgrowth and patterning in the developing embryo. *Development* **121**, 439-451.
Dahle, O., Kumar, A. and Kuehn, M. R. (2010). Nodal signaling recruits the histone demethylase Jmjd3 to counteract polycomb-mediated repression at target genes. *Sci. Signal.* **3**, ra48.
Daly, A. C., Randall, R. A. and Hill, C. S. (2008). Transforming growth factor beta-induced Smad1/5 phosphorylation in epithelial cells is mediated by novel receptor complexes and is essential for anchorage-independent growth. *Mol. Cell. Biol.* **28**, 6889-6902.
de Winter, J. P., Roelen, B. A., ten Dijke, P., van der Burg, B. and van den Eijnden-van Raaij, A. J. (1997). DPC4 (SMAD4) mediates transforming growth factor-beta1 (TGF-beta1) induced growth inhibition and transcriptional response in breast tumour cells. *Oncogene* **14**, 1891-1899.
Ding, J., Yang, L., Yan, Y. T., Chen, A., Desai, N., Wynshaw-Boris, A. and Shen, M. M. (1998). Cripto is required for correct orientation of the anterior-posterior axis in the mouse embryo. *Nature* **395**, 702-707.
Dobreva, M. P., Pereira, P. N., Deprest, J. and Zwijsen, A. (2010). On the origin of amniotic stem cells: of mice and men. *Int. J. Dev. Biol.* **54**, 761-777.
Fei, T. and Chen, Y. G. (2010). Regulation of embryonic stem cell self-renewal and differentiation by TGF-beta family signaling. *Sci. China Life Sci.* **53**, 497-503.
Furtado, M. B., Solloway, M. J., Jones, V. J., Costa, M. W., Biben, C., Wolstein, O., Preis, J. I., Sparrow, D. B., Saga, Y., Dunwoodie, S. L. et al. (2008). BMP/SMAD1 signaling sets a threshold for the left/right pathway in lateral plate mesoderm and limits availability of SMAD4. *Genes Dev.* **22**, 3037-3049.
Galvin, K. E., Travis, E. D., Yee, D., Magnuson, T. and Vivian, J. L. (2010). Nodal signaling regulates the bone morphogenic protein pluripotency pathway in mouse embryonic stem cells. *J. Biol. Chem.* **285**, 19747-19756.
Granier, C., Gurchenkov, V., Perea-Gomez, A., Camus, A., Ott, S., Papanayotou, C., Iranzo, J., Moreau, A., Reid, J., Koentges, G. et al. (2011).

Nodal cis-regulatory elements reveal epiblast and primitive endoderm heterogeneity in the peri-implantation mouse embryo. *Dev. Biol.* **349**, 350-362.
Gronroos, E., Kingston, I. J., Ramachandran, A., Randall, R. A., Vizan, P. and Hill, C. S. (2012). TGF-beta inhibits BMP-induced transcription through novel phosphorylated Smad1/5-Smad3 complexes. *Mol. Cell. Biol.* **32**, 2904-2916.
Herrmann, B. G., Labeit, S., Poustka, A., King, T. R. and Lehrach, H. (1990). Cloning of the T gene required in mesoderm formation in the mouse. *Nature* **343**, 617-622.
Hoodless, P. A., Pye, M., Chazaud, C., Labbe, E., Attisano, L., Rossant, J. and Wrana, J. L. (2001). FoxH1 (Fast) functions to specify the anterior primitive streak in the mouse. *Genes Dev.* **15**, 1257-1271.
Imamura, T., Takase, M., Nishihara, A., Oeda, E., Hanai, J., Kawabata, M. and Miyazono, K. (1997). Smad6 inhibits signalling by the TGF-beta superfamily. *Nature* **389**, 622-626.
Iratni, R., Yan, Y. T., Chen, C., Ding, J., Zhang, Y., Price, S. M., Reinberg, D. and Shen, M. M. (2002). Inhibition of excess nodal signaling during mouse gastrulation by the transcriptional corepressor DRAP1. *Science* **298**, 1996-1999.
Ishimura, A., Chida, S. and Osada, S. (2008). Man1, an inner nuclear membrane protein, regulates left-right axis formation by controlling nodal signaling in a node-independent manner. *Dev. Dyn.* **237**, 3565-3576.
Kalantry, S., Manning, S., Haub, O., Tomihara-Newberger, C., Lee, H. G., Fangman, J., Disteche, C. M., Manova, K. and Lacy, E. (2001). The amnionless gene, essential for mouse gastrulation, encodes a visceral-endoderm-specific protein with an extracellular cysteine-rich domain. *Nat. Genet.* **27**, 412-416.
Kawai, S., Faucheu, C., Gallea, S., Spinella-Jaegle, S., Atfi, A., Baron, R. and Roman, S. R. (2000). Mouse smad8 phosphorylation downstream of BMP receptors ALK-2, ALK-3, and ALK-6 induces its association with Smad4 and transcriptional activity. *Biochem. Biophys. Res. Commun.* **271**, 682-687.
Kimura, C., Yoshinaga, K., Tian, E., Suzuki, M., Aizawa, S. and Matsuo, I. (2000). Visceral endoderm mediates forebrain development by suppressing posteriorizing signals. *Dev. Biol.* **225**, 304-321.
Lawson, K. A., Dunn, N. R., Roelen, B. A., Zeinstra, L. M., Davis, A. M., Wright, C. V., Korving, J. P. and Hogan, B. L. (1999). Bmp4 is required for the generation of primordial germ cells in the mouse embryo. *Genes Dev.* **13**, 424-436.
Lechleider, R. J., Ryan, J. L., Garrett, L., Eng, C., Deng, C., Wynshaw-Boris, A. and Roberts, A. B. (2001). Targeted mutagenesis of Smad1 reveals an essential role in chorioallantoic fusion. *Dev. Biol.* **240**, 157-167.
Liu, P., Wakamiya, M., Shea, M. J., Albrecht, U., Behringer, R. R. and Bradley, A. (1999). Requirement for Wnt3 in vertebrate axis formation. *Nat. Genet.* **22**, 361-365.
Lopes Floro, K., Artap, S. T., Preis, J. I., Fatkin, D., Chapman, G., Furtado, M. B., Harvey, R. P., Hamada, H., Sparrow, D. B. and Dunwoodie, S. L. (2011). Loss of Cited2 causes congenital heart disease by perturbing left-right patterning of the body axis. *Hum. Mol. Genet.* **20**, 1097-1110.
Madabhushi, M. and Lacy, E. (2011). Anterior visceral endoderm directs ventral morphogenesis and placement of head and heart via BMP2 expression. *Dev. Cell* **21**, 907-919.
Maretto, S., Cordenonsi, M., Dupont, S., Braghetta, P., Broccoli, V., Hassan, A. B., Volpin, D., Bressan, G. M. and Piccolo, S. (2003). Mapping Wnt/beta-catenin signaling during mouse development and in colorectal tumors. *Proc. Natl. Acad. Sci. USA* **100**, 3299-3304.
Meersseman, G., Verschueren, K., Nelles, L., Blumenstock, C., Kraft, H., Wuytens, G., Remacle, J., Kozak, C. A., Tylzanowski, P., Niehrs, C. et al. (1997). The C-terminal domain of Mad-like signal transducers is sufficient for biological activity in the Xenopus embryo and transcriptional activation. *Mech. Dev.* **61**, 127-140.
Meno, C., Ito, Y., Saijoh, Y., Matsuda, Y., Tashiro, K., Kuhara, S. and Hamada, H. (1997). Two closely-related left-right asymmetrically expressed genes, lefty-1 and lefty-2: their distinct expression domains, chromosomal linkage and direct neuralizing activity in Xenopus embryos. *Genes Cells* **2**, 513-524.
Meno, C., Gritsman, K., Ohishi, S., Ohfuji, Y., Heckscher, E., Mochida, K., Shimono, A., Kondoh, H., Talbot, W. S., Robertson, E. J. et al. (1999). Mouse Lefty2 and zebrafish antivin are feedback inhibitors of nodal signaling during vertebrate gastrulation. *Mol. Cell* **4**, 287-298.
Mesnard, D., Guzman-Ayala, M. and Constam, D. B. (2006). Nodal specifies embryonic visceral endoderm and sustains pluripotent cells in the epiblast before overt axial patterning. *Development* **133**, 2497-2505.
Mine, N., Anderson, R. M. and Klingensmith, J. (2008). BMP antagonism is required in both the node and lateral plate mesoderm for mammalian left-right axis establishment. *Development* **135**, 2425-2434.
Monteiro, R. M., de Sousa Lopes, S. M., Korchynskyi, O., ten Dijke, P. and Mummery, C. L. (2004). Spatio-temporal activation of Smad1 and Smad5 in vivo: monitoring transcriptional activity of Smad proteins. *J. Cell Sci.* **117**, 4653-4663.
Moya, I. M., Umans, L., Maas, E., Pereira, P. N., Beets, K., Francis, A., Sents, W., Robertson, E. J., Mummery, C. L., Huylebroeck, D. et al. (2012). Stalk cell phenotype depends on integration of Notch and Smad1/5 signaling cascades. *Dev. Cell* **22**, 501-514.
Norris, D. P., Brennan, J., Bikoff, E. K. and Robertson, E. J. (2002). The Foxh1-dependent autoregulatory enhancer controls the level of Nodal signals in the mouse embryo. *Development* **129**, 3455-3468.
Osada, S. I., Saijoh, Y., Frisch, A., Yeo, C. Y., Adachi, H., Watanabe, M., Whitman, M., Hamada, H. and Wright, C. V. (2000). Activin/nodal responsiveness and asymmetric expression of a Xenopus nodal-related gene converge on a FAST-regulated module in intron 1. *Development* **127**, 2503-2514.
Perea-Gomez, A., Vella, F. D., Shawlot, W., Oulad-Abdelghani, M., Chazaud, C., Meno, C., Pfister, V., Chen, L., Robertson, E., Hamada, H. et al. (2002). Nodal antagonists in the anterior visceral endoderm prevent the formation of multiple primitive streaks. *Dev. Cell* **3**, 745-756.
Perea-Gomez, A., Camus, A., Moreau, A., Grieve, K., Moneron, G., Dubois, A., Cibert, C. and Collignon, J. (2004). Initiation of gastrulation in the mouse embryo is preceded by an apparent shift in the orientation of the anterior-posterior axis. *Curr. Biol.* **14**, 197-207.
Pereira, P. N., Dobreva, M. P., Graham, L., Huylebroeck, D., Lawson, K. A. and Zwijsen, A. (2011). Amnion formation in the mouse embryo: the single amniochorionic fold model. *BMC Dev. Biol.* **11**, 48.
Roelandt, P., Pauwelyn, K. A., Sancho-Bru, P., Subramanian, K., Bose, B., Ordovas, L., Vanuytsel, K., Geraerts, M., Firpo, M., De Vos, R. et al. (2010). Human embryonic and rat adult stem cells with primitive endoderm-like phenotype can be fated to definitive endoderm, and finally hepatocyte-like cells. *PLoS ONE* **5**, e12101.
Rosen, B. and Beddington, R. S. (1993). Whole-mount in situ hybridization in the mouse embryo: gene expression in three dimensions. *Trends Genet.* **9**, 162-167.
Sakuma, R., Ohnishi, Yi, Y., Meno, C., Fujii, H., Juan, H., Takeuchi, J., Ogura, T., Li, E., Miyazono, K. and Hamada, H. (2002). Inhibition of Nodal signalling by Lefty mediated through interaction with common receptors and efficient diffusion. *Genes Cells* **7**, 401-412.
Shen, M. M. (2007). Nodal signaling: developmental roles and regulation. *Development* **134**, 1023-1034.
Shi, Y. and Massague, J. (2003). Mechanisms of TGF-beta signaling from cell membrane to the nucleus. *Cell* **113**, 685-700.
Tam, P. P. and Loebel, D. A. (2007). Gene function in mouse embryogenesis: get set for gastrulation. *Nat. Rev. Genet.* **8**, 368-381.
Tanegashima, K., Haramoto, Y., Yokota, C., Takahashi, S. and Asashima, M. (2004). Xantivin suppresses the activity of EGF-CFC genes to regulate nodal signaling. *Int. J. Dev. Biol.* **48**, 275-283.
Thomas, P. and Beddington, R. (1996). Anterior primitive endoderm may be responsible for patterning the anterior neural plate in the mouse embryo. *Curr. Biol.* **6**, 1487-1496.
Tian, T. and Meng, A. M. (2006). Nodal signals pattern vertebrate embryos. *Cell Mol. Life Sci.* **63**, 672-685.
Tremblay, K. D., Dunn, N. R. and Robertson, E. J. (2001). Mouse embryos lacking Smad1 signals display defects in extra-embryonic tissues and germ cell formation. *Development* **128**, 3609-3621.
Uehara, M., Yashiro, K., Takaoka, K., Yamamoto, M. and Hamada, H. (2009). Removal of maternal retinoic acid by embryonic CYP26 is required for correct Nodal expression during early embryonic patterning. *Genes Dev.* **23**, 1689-1698.
Varlet, I., Collignon, J. and Robertson, E. J. (1997). nodal expression in the primitive endoderm is required for specification of the anterior axis during mouse gastrulation. *Development* **124**, 1033-1044.
Vincent, S. D., Dunn, N. R., Hayashi, S., Norris, D. P. and Robertson, E. J. (2003). Cell fate decisions within the mouse organizer are governed by graded Nodal signals. *Genes Dev.* **17**, 1646-1662.
Watanabe, M. and Whitman, M. (1999). FAST-1 is a key maternal effector of mesoderm inducers in the early Xenopus embryo. *Development* **126**, 5621-5634.
Willems, E. and Leyns, L. (2008). Patterning of mouse embryonic stem cell-derived pan-mesoderm by Activin A/Nodal and Bmp4 signaling requires Fibroblast Growth Factor activity. *Differentiation* **76**, 745-759.
Winnier, G., Blessing, M., Labosky, P. A. and Hogan, B. L. (1995). Bone morphogenetic protein-4 is required for mesoderm formation and patterning in the mouse. *Genes Dev.* **9**, 2105-2116.
Yamamoto, M., Meno, C., Sakai, Y., Shiratori, H., Mochida, K., Ikawa, Y., Saijoh, Y. and Hamada, H. (2001a). The transcription factor FoxH1 (FAST) mediates Nodal signaling during anterior-posterior patterning and node formation in the mouse. *Genes Dev.* **15**, 1242-1256.
Yamamoto, T. S., Takagi, C., Hyodo, A. C. and Ueno, N. (2001b). Suppression of head formation by Xmsx-1 through the inhibition of intracellular nodal signaling. *Development* **128**, 2769-2779.
Yang, L., Zhang, H., Hu, G., Wang, H., Abate-Shen, C. and Shen, M. M. (1998). An early phase of embryonic Dlx5 expression defines the rostral boundary of the neural plate. *J. Neurosci.* **18**, 8322-8330.
Yang, X., Castilla, L. H., Xu, X., Li, C., Gotay, J., Weinstein, M., Liu, P. P. and Deng, C. X. (1999). Angiogenesis defects and mesenchymal apoptosis in mice lacking SMAD5. *Development* **126**, 1571-1580.
Yum, J., Jeong, H. M., Kim, S., Seo, J. W., Han, Y., Lee, K. Y. and Yeo, C. Y. (2009). PKA-mediated stabilization of FoxH1 negatively regulates ERalpha activity. *Mol. Cells* **28**, 67-71.
Zhang, H. and Bradley, A. (1996). Mice deficient for BMP2 are nonviable and have defects in amnion/chorion and cardiac development. *Development* **122**, 2977-2986.

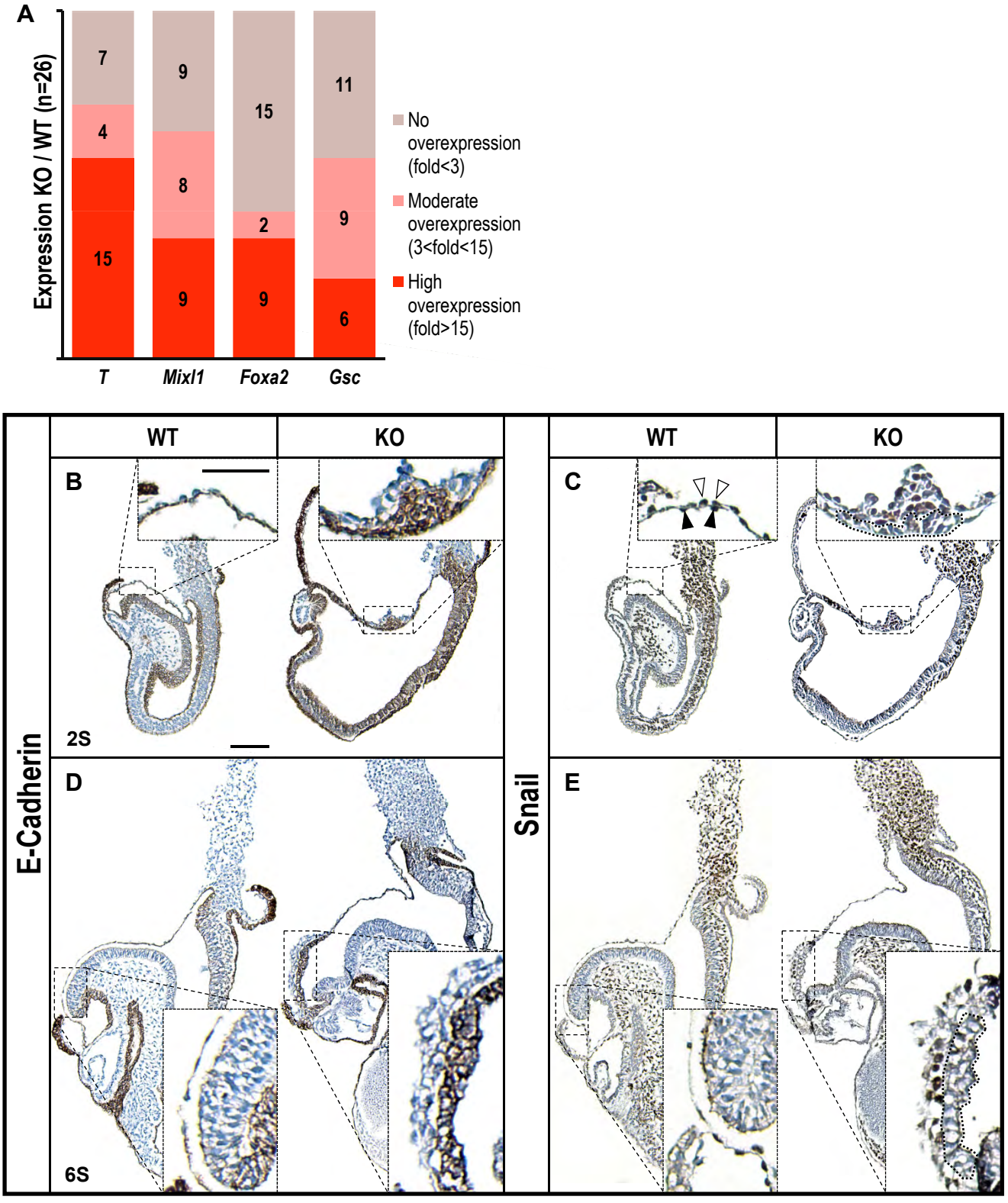

Fig. S1. Ectopic expression of mesoderm markers in the *Smad5* mutant amnion. (**A**) Bar graph summarizing the expression of *T, Mixl1*, *Gsc* and *Foxa2* by quantitative RT-PCR in *Smad5* knockout compared with control littermate amnions at E7.5 (*n*=26 amnion pairs), well before the morphological appearance of the cell clump. (**B-E**) E-cadherin and Snail localization in wild-type and *Smad5* knockout embryos at the 2S and 6S stage, respectively. Insets are magnifications of the boxed areas. In wild-type embryos, Snail is present both in the amniotic mesoderm (open arrowheads) and in the amniotic ectoderm (arrowheads). In the clump in *Smad5* KO amnion, Snail is absent from most cells located in the outlined region. Scale bars: 100 µm on figure panels; 25 µm in the insers.

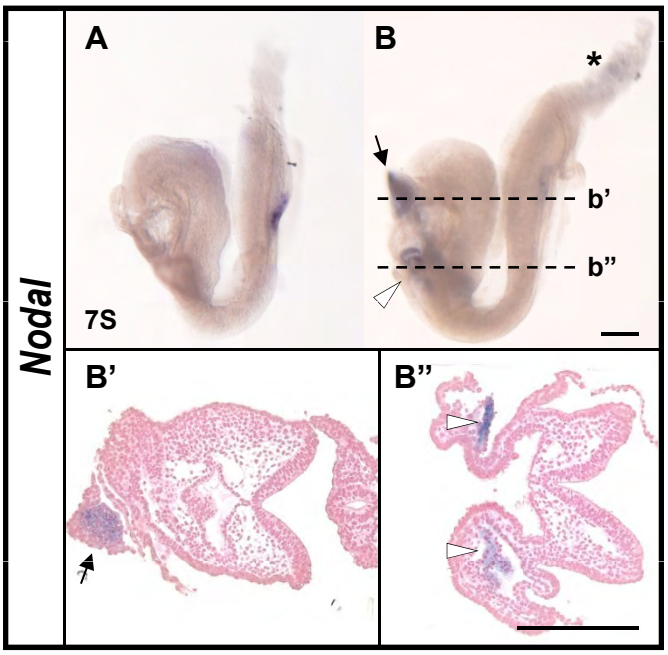

Fig. S2. Ectopic *nodal* expression in the *Smad5* mutant at E8.5. (**A**,**B**) *Nodal* expression in (A) wild-type and (B) *Smad5* KO embryos at 7S stage. Ectopic *Nodal* is expressed in amnion (arrow), cardiac crescent (open arrow head) and distal tip of the allantois (asterisk). (**B′**,**B″**) Transverse sections of the *Smad5* KO embryo shown in B at the indicated levels. Scale bars: 200 µm.

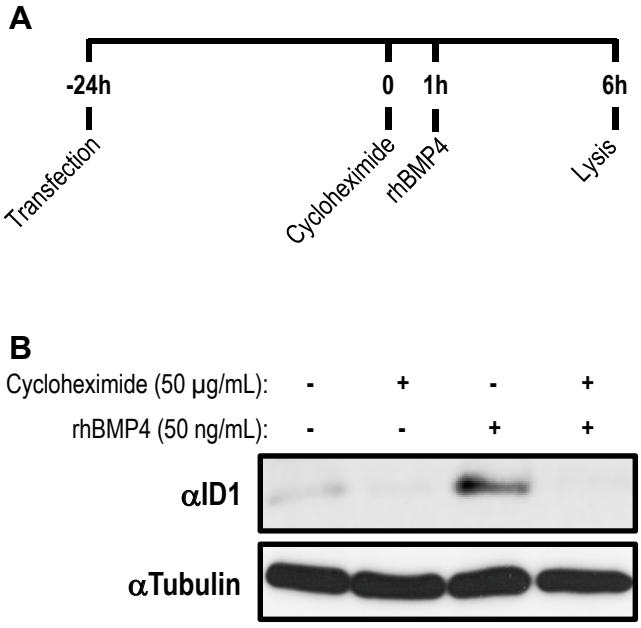

Fig. 3. Validation of protein synthesis blockade by cycloheximide. (**A**) Experimental setup using cycloheximide. Treatment of HEK293T cells with cycloheximide was for 1 hour before and during the 5-hour stimulation with rhBMP4. (**B**) Treatment with cycloheximide as depicted in A blocks effectively protein synthesis, as shown by western blot analysis of the BMP target gene ID1. Tubulin was used as a loading control.

Target Gene	Primer sequence
β-galactosidase	**TTGTTCCCACGGAGAATCCG**
	CACCACAGATGAAACGCCGA
Bmp4	**GATCACCTCAACTCAACCAA**
	TTTCAACACCACCTTGTCAT
Foxa2	**AGTCACGAACAAAGCGGG**
	TTCCTCAAAGCTCTCCCAAAG
Gapdh	**AAGAAGGTGGTGAAGCAGGC**
	GCCTCTCTTGCTCAGTGTCC
Gsc	**AGTCAGAAAACGCCGAGAAG**
	TGCAAGTAGCATCGACTGTC
Lefty2	**TCCTTGCCCATGATTGTCAG**
	CTGACGAGAGCACTAAGTTAGG
luciferase	**ACATTTCGCAGCCTACCGTAGTGT**
	GGTAATCCGTTTTAGAATCC
Mixl1	**TGGCTCAAAGTTGGACTCC**
	CAGTAAAGGCTCAGTGTCAGAG
Nodal	**AAAAGTGTTGGCATCAGCCC**
	TGGTGCTGGCGACAGGTAC
T	**AACAGCTCTCCAACCTATGC**
	TACCATTGCTCACAGACCAG
Ubc	**TAAAAAGAGCCCTCCTTGTGCT**
	AGACACCTCCCCATCACAC
Wnt3	**AGCTGCCAAGAGTGTATTCG**
	CTAGATCCTGCTTCTCATGGG
Universal primer 1	**ATATGGATCCGGCGCGCCGTCGACTTTTTTTTTTTTTTTTT**
Universal primer 2	**ATATCTCGAGGGCGCGCCGGATCCTTTTTTTTTTTTTTTTT**

Table S1. **Validated primers used for quantitative RT-PCR.** The primer sequences of the respective genes and poly-dT universal primers appear with the forward primer followed by the reverse primer.